Molecular Therapy
Nucleic Acids
Original Article

MicroRNA-126 Regulates Angiogenesis and Neurogenesis in a Mouse Model of Focal Cerebral Ischemia

Meijie Qu,[1,5,6] Jiaji Pan,[2,5] Liping Wang,[1] Panting Zhou,[2] Yaying Song,[1] Shuhong Wang,[3] Lu Jiang,[2] Jieli Geng,[4] Zhijun Zhang,[2] Yongting Wang,[2] Yaohui Tang,[2] and Guo-Yuan Yang[1,2]

[1]Department of Neurology, Ruijin Hospital, School of Medicine, Shanghai Jiao Tong University, Shanghai 200025, China; [2]Med-X Research Institute and School of Biomedical Engineering, Shanghai Jiao Tong University, Shanghai 200030, China; [3]Department of Geriatrics, Ruijin Hospital, School of Medicine, Shanghai Jiao Tong University, Shanghai 200025, China; [4]Department of Neurology, Shanghai Renji Hospital, School of Medicine, Shanghai Jiao Tong University, Shanghai 200127, China

Studies demonstrate that microRNA-126 plays a critical role in promoting angiogenesis. However, its effects on angiogenesis following ischemic stroke are unclear. Here, we explored the effect of microRNA-126-3p and microRNA-126-5p on angiogenesis and neurogenesis after brain ischemia. We demonstrated that both microRNA (miRNA)-126-3p and microRNA-126-5p increased the proliferation, migration, and tube formation of human umbilical vein endothelial cells (HUVECs) compared with the scrambled miRNA control ($p < 0.05$). Transferring microRNA-126 into a mouse middle cerebral artery occlusion model via lentivirus, we found that microRNA-126 overexpression increased the number of $CD31^+/BrdU^+$ (5-bromo-2′-deoxyuridine-positive) proliferating endothelial cells and $DCX^+/BrdU^+$ neuroblasts in the ischemic mouse brain, improved neurobehavioral outcomes ($p < 0.05$), and reduced brain atrophy volume ($p < 0.05$) compared with control mice. Western blot results showed that AKT and ERK signaling pathways were activated in the lentiviral-microRNA-126-treated group ($p < 0.05$). Both PCR and western blot results demonstrated that tyrosine-protein phosphatase non-receptor type 9 (PTPN9) was decreased in the lentiviral-microRNA-126-treated group ($p < 0.05$). Dual-luciferase gene reporter assay also showed that *PTPN9* was the direct target of microRNA-126-3p and microRNA-126-5p in the ischemic brain. We demonstrated that microRNA-126-3p and microRNA-126-5p promoted angiogenesis and neurogenesis in ischemic mouse brain, and further improved neurobehavioral outcomes. Our mechanistic study further showed that microRNA-126 mediated angiogenesis through directly inhibiting its target PTPN9 and activating AKT and ERK signaling pathways.

INTRODUCTION

Stroke is one of the leading causes of mortality and morbidity worldwide.[1] Currently, only tissue plasminogen activator (tPA) is proven as an effective drug treatment clinically.[2] However, due to a limited time window and high hemorrhagic risk, only 1%–2% of patients have benefitted from this treatment.[3] There is a critical need to develop new strategies for stroke therapy improvement.

Poor blood flow-induced cell death is the main pathology of stroke.[4] Blood flow restoration could be a potential therapeutic strategy for treating ischemic stroke.[5] Angiogenesis has been demonstrated as a significant event that resulted in brain microvasculature changes following cerebral ischemia. Previous reports have shown that angiogenesis occurred 7 and 14 days after ischemia in rodents and occurred in human brain as early as 3 days following ischemic insult.[6–8] In addition, clinical observation demonstrated a strong correlation between neovascularization and functional recovery, suggesting that newly formed vessels contributed to behavioral outcomes after ischemic stroke.[9]

Gene-based or stem cell-based therapy could improve neurobehavioral outcomes and reduce ischemic brain injury by promoting angiogenesis.[6,10,11] Our previous studies demonstrated that netrin-1 (NT-1) and stromal cell-derived factor-1 (SDF-1) overexpression increased angiogenesis in ischemic mouse brains.[11–14] Although exogenous angiogenic genes increased angiogenesis in experimental cerebral ischemia models, several disadvantages limited its clinical translation. First, gene was transferred to animals before ischemic insult, which was not acceptable for clinical application.[7,11,15] Second, many angiogenic factors were large molecules and difficult to cross the blood-brain barrier (BBB).[16] Stem cell-based therapy also showed great potential for promoting angiogenesis. Mesenchymal stem cells (MSCs) enhanced focal angiogenesis by increasing the levels of endogenous vascular endothelial growth factor (VEGF) and vascular endothelial growth factor receptor 2 (VEGFR2) in the ischemic perifocal region.[17] Endothelial progenitor cells (EPCs)

Received 4 June 2018; accepted 5 February 2019;
https://doi.org/10.1016/j.omtn.2019.02.002.

[5]These authors contributed equally to this work.

[6]Present address: Department of Neurology, The Affiliated Hospital of Qingdao University, Qingdao University, Qingdao 266000, China

Correspondence: Yaohui Tang, Med-X Research Institute and School of Biomedical Engineering, Shanghai Jiao Tong University, Shanghai 200030, China.
E-mail: yaohuitang@sjtu.edu.cn
Correspondence: Guo-Yuan Yang, Med-X Research Institute and School of Biomedical Engineering, Shanghai Jiao Tong University, Shanghai 200030, China.
E-mail: gyyang@sjtu.edu.cn

promoted neurovascular repair and improved long-term neurobehavioral outcomes by the SDF-1/C-X-C chemokine receptor type 4 (CXCR4) signaling pathway.[18] Despite these promising initial results, its therapeutic efficiency is still low due to poor cell survival.[19] Thus, there is a critical need to develop novel strategies to improve angiogenesis after cerebral ischemia.

MicroRNAs (miRNAs) were important biological factors because they could cross the BBB and target multiple angiogenesis-associated genes.[16] Various miRNAs' angiogenic function has been tested. Our previous studies showed that miRNA-210 overexpression promoted angiogenesis by upregulating brain-derived neurotrophic factor (BDGF).[20] miRNA-126, the most abundant miRNA in endothelial cells, was reported to play a vital role in angiogenesis. miRNA-126 possesses two mature strands: miRNA-126-3p and miRNA-126-5p.[21] Studies showed miRNA-126-3p promoted angiogenesis in rat heart by activating mitogen-activated protein kinase (MAPK) and AKT signaling pathways.[22] Injection of exosomes that derived from miRNA-126-3p-overexpressing adipose-derived stem cells prevented myocardial injury by protecting myocardial cells from apoptosis, inflammation, fibrosis, and increased angiogenesis.[23] However, whether miRNA-126 could promote angiogenesis after stroke remains largely unexplored.

In this study, we explored the effects of miRNA-126 in angiogenesis after ischemic stroke and its downstream target. In addition, we also tested the function of miRNA-126 in neurogenesis, and whether such increased angiogenesis and neurogenesis could further improve behavioral outcomes in adult ischemic mice.

RESULTS

LV-miRNA-126-3p and LV-miRNA-126-5p Transduction Increased miRNA-126 Expression in HUVECs

To determine the effects of miRNA-126-3p and miRNA-126-5p on the function of human umbilical vein endothelial cells (HUVECs), HUVECs were transduced with lentiviral vector carrying miRNA-126-3p, miRNA-126-5p, miRNA-126-3p sponge, or miRNA-126-5p sponge (Figure S1A). Flow cytometry analysis showed that about 70% of HUVECs were transduced with lentivirus (Figure S1B). Real-time PCR analysis showed that miRNA-126-3p and miRNA-126-5p expression were upregulated in HUVECs transduced with lentiviral-miRNA-126-3p (LV-miRNA-126-3p) and miRNA-126-5p (Figure S1C). Interestingly, the expression of miRNA-126-3p and miRNA-126-5p were comparable in HUVECs transduced with LV-miRNA-126-3p sponge, miRNA-126-5p sponge, and LV-GFP sponge (Figure S1C), suggesting transduction of miRNA-126-3p and miRNA-126-5p sponge blocked the binding between miRNA-126-3p and miRNA-126-5p and their target genes, rather than degrading miRNAs.

miRNA-126-3p and miRNA-126-5p Overexpression Promoted HUVEC Proliferation, Migration, and Tube Formation

To detect the effects of miRNA-126-3p and miRNA-126-5p on the function of HUVECs, we examined the proliferation and migration of HUVECs transduced with LV-miRNA-126-3p and LV-miRNA-126-5p. We found that both miRNA-126-3p and miRNA-126-5p overexpression promoted HUVEC proliferation and migration; inhibiting miR-126-3p and miRNA-126-5p reversed these functions (Figures S2A and S2B; $p < 0.05$). We further examined tube formation in the miRNA-126-3p or miRNA-126-5p transduced HUVECs. Results showed that both miRNA-126-3p and miRNA-126-5p overexpression promoted HUVEC tube formation, and inhibiting miR-126-3p and miRNA-126-5p reversed these cells' function (Figure S2C; $p < 0.05$). It was noted that miRNA-126-3p transduction significantly increased tube formation of HUVECs compared with the miRNA-126-5p transduced group (Figure S2C; $p < 0.05$). Meanwhile, miR-126-3p sponge transduction significantly decreased HUVEC tube formation compared with the miR-126-5p sponge transduced group (Figure S2C; $p < 0.05$).

miRNA-126 Overexpression Reduced Brain Atrophy Volume and Improved Neurobehavioral Recovery in Ischemic Mice

We first examined miRNA-126-3p and miRNA-126-5p expression in an infarct border zone of ischemic mouse brain at 1, 3, 7, and 14 days after middle cerebral artery occlusion (MCAO). miRNA was isolated from the ipsilateral hemisphere of ischemic mice (infarct hemisphere), including cortex and striatum. miRNA-126-3p and miRNA-126-5p expression were significantly decreased from days 3 to 14 after MCAO (Figure 1A). To determine the effects of miRNA-126 on the ischemic brain injury, we injected lentiviral vector carrying miRNA-126 into the mouse brain, and animals were sacrificed 2 and 3 weeks after lentiviral vector injection for histological and biological analysis (Figure 1B). Fluorescent imaging showed GFP successfully expressed in ischemic mouse brain 2 and 3 weeks after lentiviral vector injection, and lentivirus-carrying miRNA-126 transfected both neurons and endothelial cells (Figure S4). Our PCR results demonstrated that miRNA-126 expression was upregulated in both cortex and striatum of ischemic mice (Figures 1C and 1D). We also found that a cavity was detected in mouse brain at 3 and 4 weeks after permanent middle cerebral artery occlusion (pMCAO) even without any virus treatment (Figure S3), suggesting an MCAO injury-induced cavity was formed in the mouse brain. We further evaluated whether miRNA-126 overexpression could reduce infarct volume and improve neurobehavioral recovery. Cresyl violet staining showed that atrophy volume was significantly decreased in the LV-miRNA-126 transduced group compared with the control group (Figure 1E; $p < 0.05$), and miRNA-126 overexpression significantly reduced neurological deficits and improved behavioral recovery, as shown by modified neurological severity scores (mNSSs) and rotarod test (Figure 1F; $p < 0.05$).

miRNA-126 Overexpression Promoted Angiogenesis and Neurogenesis *In Vitro*

To explore the effects of miRNA-126 on angiogenesis, we measured the length and diameter of blood vessels in ischemic mice brain transduced by lentiviral vector. Our results demonstrated that overexpression of miRNA-126 significantly increased the length and

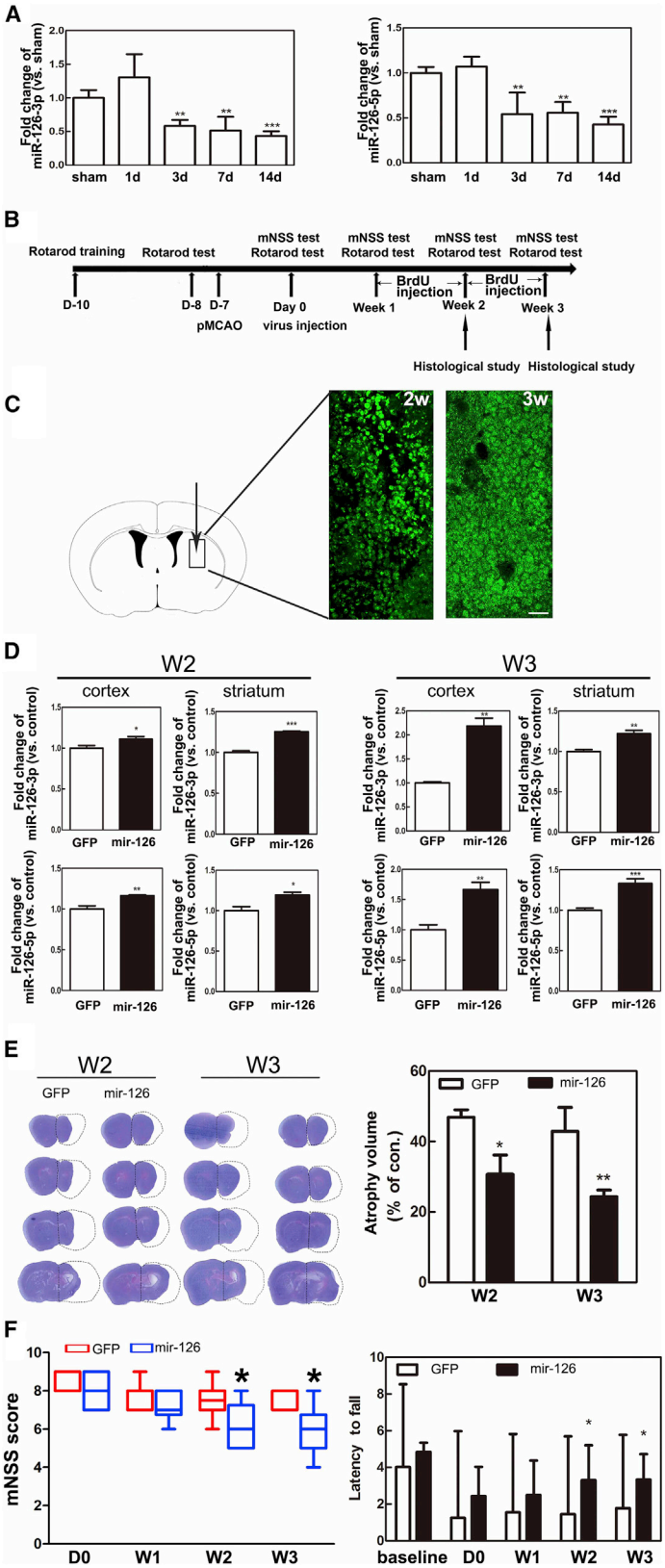

Figure 1. Overexpression of miRNA-126 Reduced Brain Atrophy Volume and Improved Neurobehavioral Recovery in Ischemic Mice

(A) Bar graph revealed the expression of miRNA-126-3p and miRNA-126-5p in brain tissue of the sham group and pMCAO group at 1, 3, 7, and 14 days after ischemia. n = 3 per group. (B) Diagram of experimental design. (C) Fluorescent imaging showed GFP expression in ischemic mouse brain at 2 and 3 weeks after lentiviral vector injection. Scale bar, 250 μm. (D) Real-time PCR showed miRNA-126 expression in cortex and striatum of ischemic mice at 2 and 3 weeks after lentiviral vector injection. n = 6 per group. (E) Representative photomicrographs of coronal sections stained by cresyl violet for evaluation and quantification of brain atrophy. n = 6 per group. (F) Bar graphs summarized the results of mNSS evaluation and rotarod test in LV-miRNA-126- and LV-GFP-treated groups. n = 8–10 per group. Data were presented as median ± 95% confidence interval. *p < 0.05; **p < 0.01; ***p < 0.001.

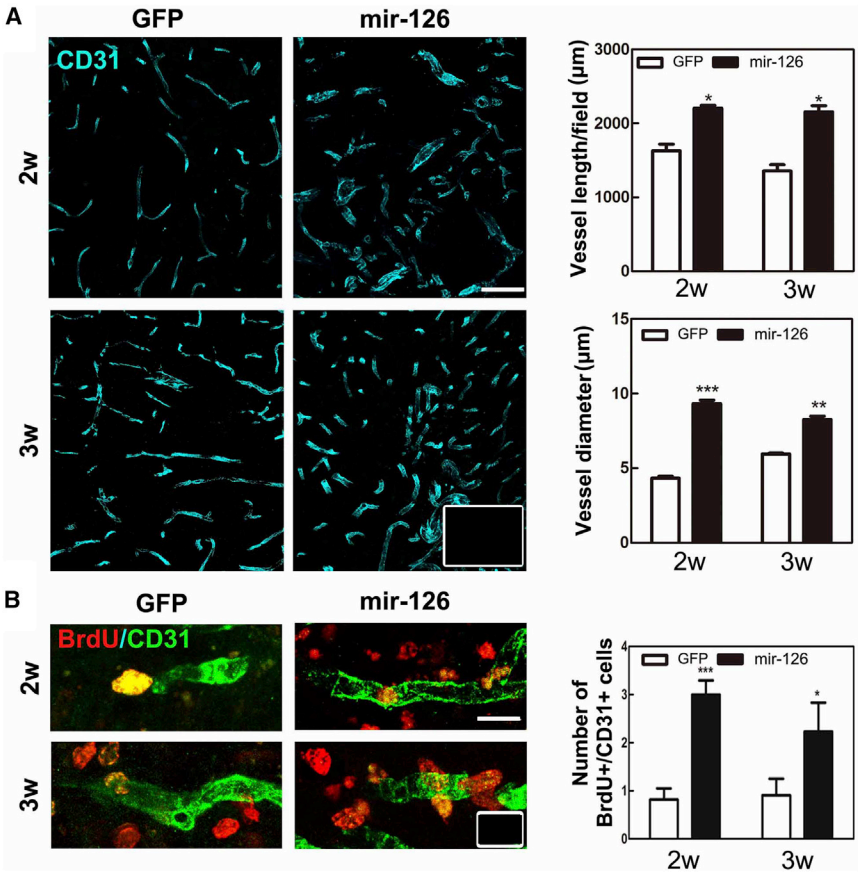

Figure 2. miRNA-126 Promoted Angiogenesis and Vessel Remodeling in Ischemic Mice

(A) Photomicrographs showed cluster of $CD31^+$ microvessels in the ipsilateral hemisphere after pMCAO in LV-GFP and LV-miRNA-126 groups. Bar graphs showed the length and diameter of vessels in the ipsilateral hemisphere of ischemic mice at 2 and 3 weeks after lentiviral vector injection. Scale bar, 50 μm. n = 5 per group. (B) Representative photomicrographs showed CD31 and BrdU double-positive cells in ischemic mice. Bar graphs showed the number of $CD31^+/BrdU^+$ cells in the ipsilateral hemisphere. Scale bar, 12.5 μm. Inserted box indicated staining result using isotype-matched IgG control. n = 5 per group. Data were presented as mean ± SD. $^*p < 0.05$; $^{**}p < 0.01$; $^{***}p < 0.001$.

diameter of blood vessels, compared with the GFP group at 2 and 3 weeks after lentiviral vector injection (Figure 2A). In addition, overexpression of miRNA-126 substantially increased the number of 5-bromo-2′-deoxyuridine-positive ($BrdU^+$)/$CD31^+$ cells in the peri-focal region at 2 and 3 weeks after lentiviral vector injection, compared with the GFP group (Figure 2B). These results indicated that miRNA-126 promoted vessel remodeling and angiogenesis after cerebral ischemia.

To explore whether miRNA-126 promoted neurogenesis, we performed doublecortin (DCX)/BrdU double staining. As shown in Figure 3, miRNA-126 overexpression significantly increased the number of $DCX^+/BrdU^+$ cells in the subventricular zone (SVZ) at 2 and 3 weeks and in the perifocal region at 3 weeks after lentiviral vector injection, suggesting that miRNA-126 promoted neurogenesis.

PTPN9 Was the Direct Downstream Target Gene of miRNA-126

To explore the underlying mechanism of miRNA-126 in angiogenesis and neurogenesis, we examined phosphorylation of AKT and ERK. Protein was isolated from the ipsilateral hemisphere of the brain including cortex and striatum. Western blot results showed miRNA-126 overexpression significantly elevated the expression of p-AKT and p-ERK in the ischemic mouse brain, compared with the control group (Figure 4).

We then examined the expression of downstream genes of miRNA-126-3p and miRNA-126-5p, including *DUSP10*, *SPRED1*, *PTPN9*, *PTPN7*, and *PIK3R2*, which were all related to AKT and ERK signaling pathways. RNA was isolated from the ipsilateral hemisphere of the brain, including cortex and striatum. Our real-time PCR results demonstrated that *PTPN9*, *SPRED1*, and *PIK3R2* were significantly decreased 2 and 3 weeks after LV-miRNA-126 treatment, and β-actin was used as a housekeeper (Figures 5A–5E). By searching miRNA-126-3p and miRNA-126-5p seed sequence and mice *PTPN9* 3′ UTR, we found that *PTPN9* 3′ UTR was complementary to nucleotides 2–7 of the miRNA-126-5p sequence and nucleotides 2–8 of the miRNA-126-3p sequence (Figure 5F). Our western blot results further demonstrated that miRNA-126-3p and miRNA-126-5p inhibited PTPN9 expression (Figures 5G and 5H). The experimental and matching results illustrated *PTPN9* might be a potential target of both miRNA-126-3p and miRNA-126-5p in mice. Further studies showed that overexpression of miR-126 reduced PTPN9 in neurons (Figures S6A–S6C). To confirm whether PTPN9 was the direct target of miRNA-126-3p and miRNA-126-5p, we cloned *PTPN9* mRNA 3′ UTR fragment to a luciferase reporter plasmid containing the putative miRNA-126-3p and miRNA-126-5p binding sites. Luciferase reporter plasmid and miRNA mimic were co-transfected in 293T cells. Luciferase activity level was reduced in the cells co-transfected with miRNA-126-3p/miRNA-126-5p mimic and *PTPN9* mRNA 3′ UTR fragment group, compared with the mimic control and the *PTPN9* 3′ UTR fragment group (Figure 5I).

DISCUSSION

Angiogenesis plays an important role in improving neurobehavioral recovery after stroke.[24] In the present study, we explored the function of miRNA-126-3p and miRNA-126-5p in angiogenesis using *in vitro* and *in vivo* models. We found that overexpression of both miRNA-126-3p and miRNA-126-5p promoted the proliferation, migration,

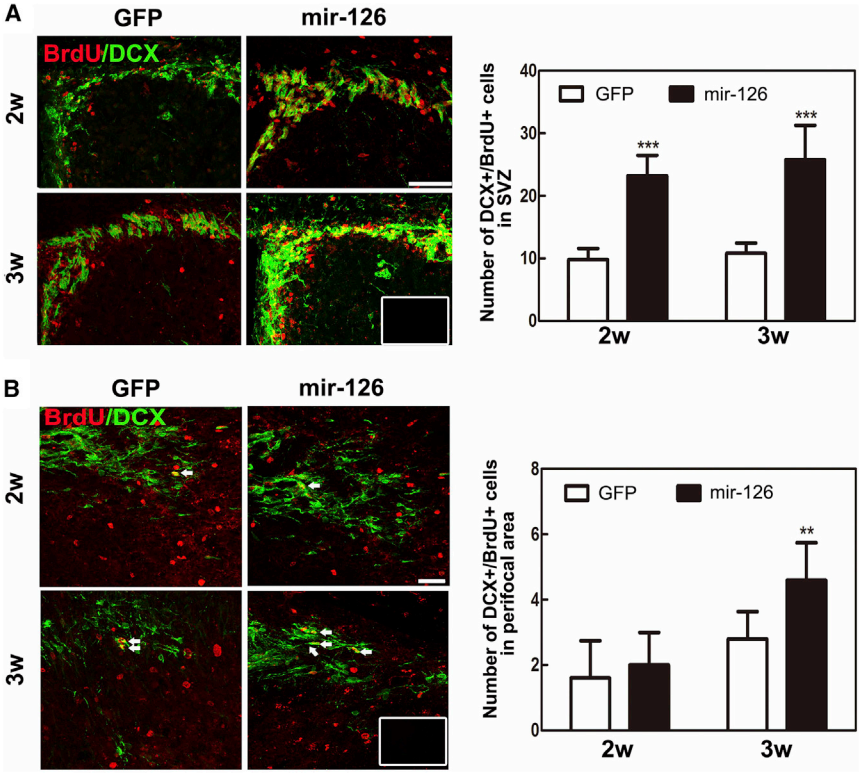

Figure 3. miRNA-126 Promoted Neurogenesis in Ischemic Mouse Brain

(A) Double immunostaining of DCX^+ and $BrdU^+$ cells and quantification of $DCX^+/BrdU^+$ cells in the SVZ after lentiviral vector injection. n = 5 per group. Scale bar, 50 μm. (B) Double immunostaining of DCX^+ and $BrdU^+$ cells and quantification of $DCX^+/BrdU^+$ cells in the perifocal region of the ipsilateral hemisphere after lentiviral vector injection. Inserted box indicated staining result using isotype-matched IgG control. n = 5 per group. Scale bar, 50 μm. Data were presented as mean ± SD. $^{**}p < 0.01$; $^{***}p < 0.001$.

and tube formation of HUVECs; contributed to angiogenesis and neurogenesis in the ischemic mice brain; and further improved behavioral recovery by downregulating PTPN9 and activating AKT and ERK signaling pathways.

It has been well documented that miRNA-126 was critically involved in regulating angiogenesis. However, the effects of miRNA-126-3p and miRNA-126-5p on angiogenesis are still controversial. Zhou et al.[25] demonstrated different effects of miRNA-126-5p and miRNA-126-3p on angiogenesis using different models. They found that inhibition of miRNA-126-3p in the laser injury-induced choroidal neovascularization (CNV) model repressed neovascularization. In the study, anti-miR-126-3p, anti-miR-126-5p, or a scramble control was subretinally injected into the eye immediately following laser injury in three locations and regressed neovascularization at postinjury days 3 and 7. However, silencing of miR-126-5p did not significantly impact neovascularization. In addition, they found that injection of miR-126-3p mimic subretinally after laser injury led to ~60% decrease in neovascularization, whereas miR-126-5p mimic significantly but mildly enhanced laser-induced neovascularization. They further used HUVEC as an *in vitro* model to dissect the roles of miR-126-3p and miR-126-5p on angiogenesis. Under starvation condition, miR-126-5p, but not miR-126-3p, significantly increased proliferation and migration of HUVECs *in vitro*, which is different from the *in vivo* data.[25] Conversely, Cao et al.[26] illustrated miRNA-126-3p overexpression promoted HUVEC migration and tube formation, and injection of 2.5 μg of miRNA-126-3p into hindlimb 2 weeks after femoral artery ligation increased microvascular perfusion and vascular density of the ischemic hindlimb, but they did not detect the function of miRNA-126-5p. In our study, we tested and compared the function of both miRNA-126-3p and miRNA-126-5p on angiogenesis by evaluating proliferation, migration, and tube formation of HUVECs. We found overexpression of both miRNA-126-3p and miRNA-126-5p significantly increased the proliferation, migration, and tube formation of HUVECs. Interestingly, miRNA-126-3p showed better effects on tube formation, which is different from Zhou et al.'s[25] study. Taken together, all of the studies suggested that the role of miR-126 in angiogenesis depends on cell type, animal model, and strand of miR-126.

The majority of patients still suffer from various long-term neurological deficits, even though they survive after timely treatment in the acute phase of ischemic stroke.[27] One of the major issues is limited angiogenesis and neurogenesis in the post-acute phase.[12] Therapeutic strategies that focus on improving angiogenesis and neurogenesis in the post-acute phase would be beneficial for improving functional recovery after stroke.[10] Previous studies showed that miRNA-126-3p promoted cardiac angiogenesis by directly downregulating SPRED1 and PIK3R2 and indirectly regulating the VEGF pathway.[22] Mathiyalagan et al.'s[28] study demonstrated that exosomes derived from $CD34^+$ cells repaired ischemic hindlimb, but knocking down miRNA-126-3p abolished their angiogenic activity and beneficial function both *in vitro* and *in vivo*. MSCs modified with miRNA-126-3p released angiogenic factors and activated Notch ligand Delta-like-4, enhancing ischemic angiogenesis in cardiac reparation.[29] However, the angiogenic and neurogenic effects of miRNA-126 in stroke have never been explored. In this study, we overexpressed miRNA-126 in the peri-infarct area of ischemic mice 1 week after stroke. Our results showed that expression of miRNA-126-3p and miRNA-126-5p was increased 2 and 3 weeks after lentiviral vector injection, and such upregulated miRNA-126 promoted angiogenesis and neurogenesis.

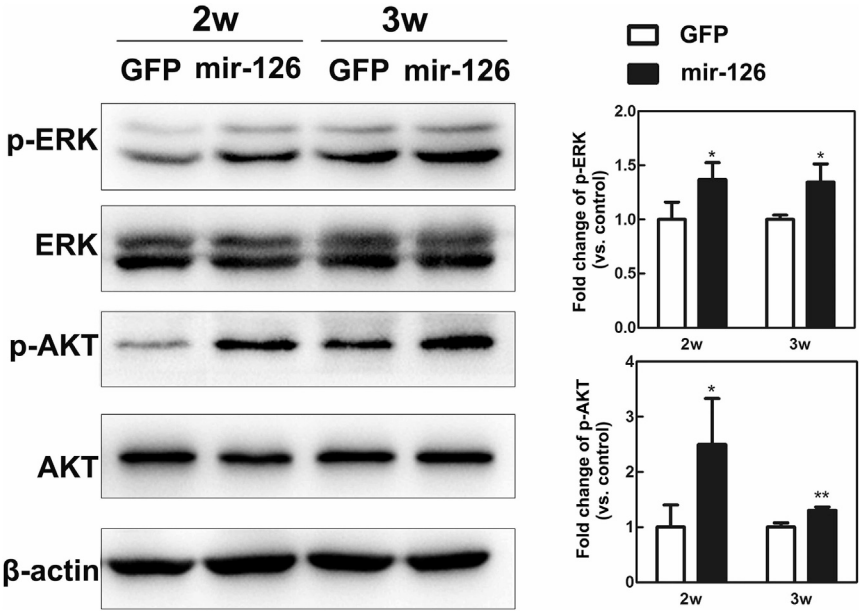

Figure 4. miRNA-126 Activated AKT and ERK Signaling Pathways in pMCAO Mice

(Left) Western blot results showed expression of p-ERK and p-AKT in ischemic mouse brain at 2 and 3 weeks after lentiviral vector injection. (Right) Quantification data from left panel. n = 5 per group. Data were presented as mean ± SD. *p < 0.05; **p < 0.01.

In our study, miRNA-126 treatment promoted the proliferation of few endothelial cells; however, we also found that injection of miRNA-126 increased the vessel length and vessel diameter, suggesting miRNA-126 is beneficial for promoting vascular remodeling, rather than only promoting angiogenesis. And such miRNA-126-mediated vascular remodeling contributed to behavioral recovery of mice subjected to stroke, suggesting miR-126 treatment holds biological relevance to the overall recovery of the animals.

It was noted that higher expression of miRNA-126 was achieved at 3 weeks after lentiviral vector injection than 2 weeks. However, no significant difference of angiogenesis and neurogenesis was observed between 2 and 3 weeks following lentiviral vector injection, suggesting the effects of miRNA-126 in angiogenesis was already saturated at the second week, and increasing the level of miRNA-126 at week 3 could not further promote its angiogenic and neurogenic effects.

miRNA-126-mediated neurovascular remodeling was beneficial for reducing brain atrophy volume and improving neurological outcomes. Recent findings suggested that strategies to enhance angiogenesis and neurogenesis for brain injuries may provide promising opportunities to improve clinical outcomes during brain functional recovery.[30] Newly formed blood vessels removed necrotic tissue and provided trophic factors.[31] Neurogenesis increased the neuroblasts proliferation, neural stem cells recruitment, and their neuronal differentiation, leading to long-term improvement of neurological function.[32–34]

Studies demonstrated that miRNA-126 activated AKT and ERK signaling pathways,[35] which are associated with angiogenesis and neurogenesis.[36–38] Previous studies showed that miRNA-126 activated AKT and ERK signaling pathways by directly binding with PIK3R2 and SPRED1, and upregulated SDF-1 expression to elevate the migration of stem cells.[35,39] We found these pathways were also activated after miRNA-126 treatment. To explore the downstream target of miRNA-126, PTPN9 was chosen as a potential downstream target of miRNA-126. PTPN9 is a member of the protein tyrosine phosphatase (PTP) family and inhibits the phosphorylation of AKT and ERK.[40,41] In addition, previous study showed that overexpression of PTPN9 reduces MAPK and AKT signaling activation, resulting in decreased glioma cell viability.[42] Studies showed PTPN9 was expressed in endothelial cell and modulated endothelial cell function.[43] It has been also demonstrated as an inhibitor of angiogenesis by negatively regulating VEGFR2 and downregulating AKT and MAPK signaling pathways.[40–42] In our study, we found PTPN9 expression was significantly decreased in miRNA-126-treated mice. Comparing miRNA-126-3p and miRNA-126-5p seed sequence with 3′ UTR of mice *PTPN9*, we found that *PTPN9* 3′ UTR exactly matched to positions 2–8 of mature miRNA-126-3p and positions 2–7 of mature miRNA-126-5p. Furthermore, luciferase gene reporter assay confirmed mice *PTPN9* was the direct target gene of miRNA-126-3p and miRNA-126-5p. It is noted that in our study the change of PTPN9 level does not reflect the change of miR-126 expression, probably because stroke itself induces more PTPN9 expression at week 3 than week 2, or miR-126 has multiple targets and PTPN9 is one of them.

In summary, our study suggested that overexpression of miRNA-126 is beneficial for promoting angiogenesis and neurogenesis, and improving neurobehavioral recovery of ischemic mice, by directly modulating its downstream target *PTPN9* (Figure 6).

MATERIALS AND METHODS

Animal Experiments

Two-month-old adult male ICR mice (n = 60) weighing 28–32 g were used in our study. Experimental animal studies were performed in accordance with the Animal Research: Reporting of *In Vivo* Experiments (ARRIVE) guidelines with government approval by the State Agency for Nature, Environment and Consumer Protection North Rhine-Westphalia. The procedures for the use of laboratory animals were approved by the Institutional Animal Care and Use Committee (IACUC) of Shanghai Jiao Tong University, China. During animal studies, the regulation for the Administration of Affairs concerning experimental animals in China enacted in 1988 were followed.

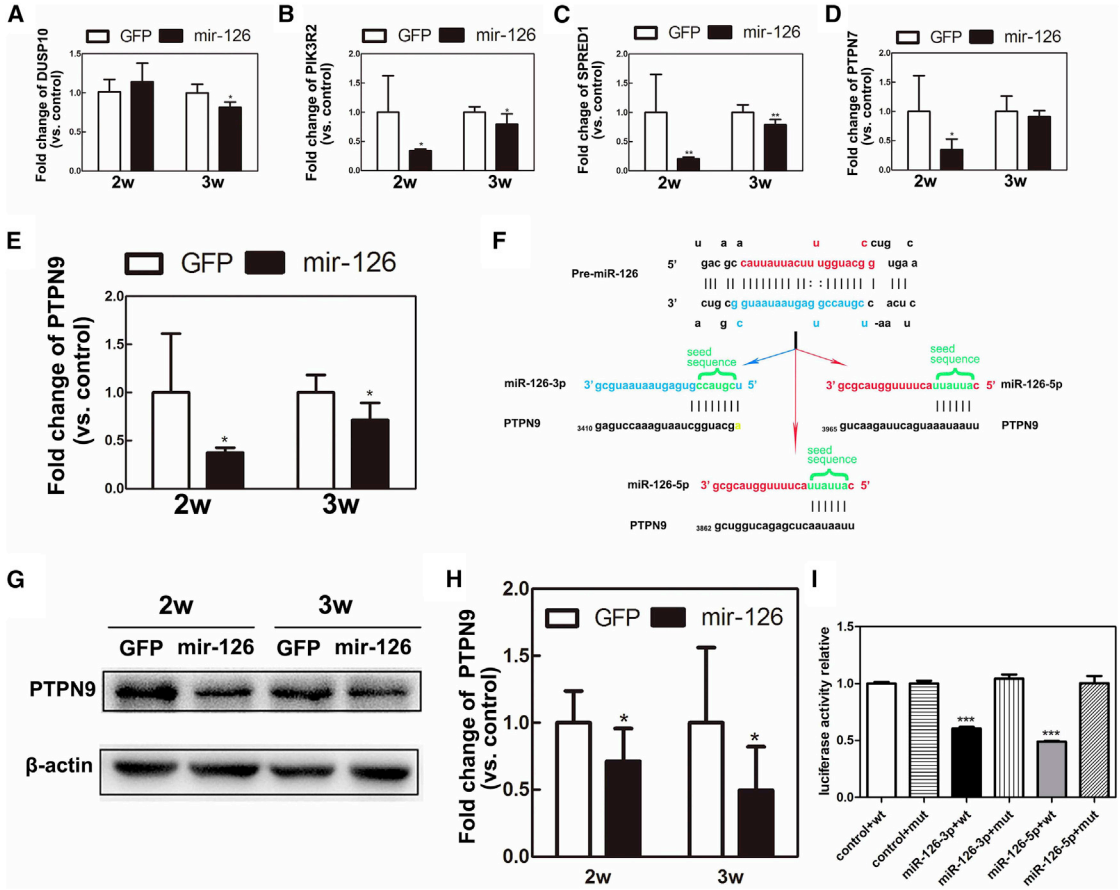

Figure 5. miRNA-126 Overexpression Inhibited Tyrosine-Protein Phosphatase Non-receptor Type 9

(A–E) Real-time PCR showed expression of (A) *DUSP10*, (B) *PIK3R2*, (C) *SPRED1*, (D) *PTPN7*, and (E) *PTPN9* in ischemic mice at 2 and 3 weeks after lentiviral vector injection. n = 5 per group. (F) The 3′ UTR of the *PTPN9* gene contains binding sites for both miRNA-126-3p and miRNA-126-5p according to bioinformatic analysis. (G) Western blot showed the expression of PTPN9 in ischemic mice at 2 and 3 weeks after lentiviral vector injection. (H) Quantification data from (G). n = 5 per group. (I) Bar graph represented luciferase activity in control plus PTPN9, control plus mutant PTPN9, miRNA-126-3p plus PTPN9, miRNA-126-3p plus mutant PTPN9, miRNA-126-5p plus PTPN9, and miRNA-126-5p plus mutant PTPN9. n = 3 per group. Data were presented as mean ± SD. *p < 0.05; **p < 0.01; ***p < 0.001.

Mice were anesthetized by ketamine and xylazine (100/10 mg/kg; Sigma-Aldrich, St. Louis, MO, USA). MCAO was performed as described previously.[44] Left common carotid artery, internal carotid artery, and external carotid artery were carefully isolated. A 6–0 nylon suture (Covidien, Mansfield, MA, USA) coated with silica was gently inserted from the external carotid artery stump to the internal carotid artery and occluded the origin of the middle cerebral artery (MCA). Body temperature was maintained at 37°C ± 0.5°C throughout the surgery using a heating pad (RWD Life Science, Shenzhen, China). Successful occlusion was verified by a Laser Doppler Flowmetry (Moor Instruments, Axminster, Devon, UK). The overall mortality rate was 20% in the study.

Lentiviral Vector Construction and Production

Plasmids of LV-miRNA-126-3p, LV-miRNA-126-5p, LV-miRNA-126, LV-miRNA-126-3p sponge, and LV-miRNA-126-5p sponge were constructed (ObiO, Shanghai, China). These plasmids were transfected into 293T cells with VSVG and p delta plasmid by calcium phosphate precipitation. 293T cells were switched to virus production medium containing Ultraculture (Lonza, Basel, Switzerland), penicillin and streptomycin (Millipore, Temecula, CA, USA), sodium pyruvate (GIBCO, Carlsbad, CA, USA), and sodium butyrate (Sinopharm chemical reagent, Shanghai, China) for 24 h. The supernatant was collected at 48 and 72 h after transfection. The viral vector was purified by 20% sucrose density gradient ultracentrifugation at 28,000 rpm for 2 h. Lentiviral vector carrying GFP was simultaneously prepared as a control.[45]

Viral Vector Transduction

HUVECs were transduced with 2.8 × 10^6 particles of LV-miRNA-126-3p, LV-miRNA-126-5p, LV-GFP, LV-miRNA-126-3p sponge, LV-miRNA-126-5p sponge, and LV-GFP sponge (MOI = 10) at 80% confluence. Medium was changed 24 h after transduction. Cells were harvested 72 h after transduction. Transduction efficiency was

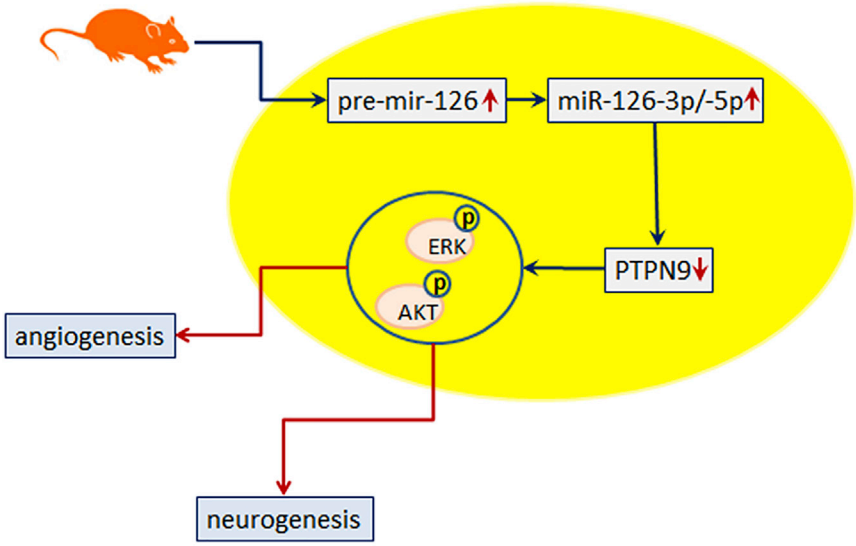

Figure 6. miRNA-126 Promotes Angiogenesis by Inhibiting PTPN9 and Activating AKT and ERK Signaling Pathways

miRNA-126-3p and miRNA-126-5p decreased after pMCAO. Transducing LV-miRNA-126 increased miRNA-126-3p/5p in the ischemic hemisphere. PTPN9 was degraded by miRNA-126-3p/5p, and thus activated AKT and ERK signal pathways and promoted angiogenesis.

analyzed by counting GFP-positive cells 72 h after transduction using flow cytometer.[45] Proliferation and migration assay were carried out 72 h after virus transfection.

Proliferation Assay

HUVECs were treated with 10 μM BrdU (Sigma, Saint Louis, MO, USA) for 6 h. For BrdU staining, cells were fixed with 4% paraformaldehyde and then treated with 0.3% Triton X-100 in PBS, 1N HCl, and 2N HCl solution for 10 min at 37°C. After blocking with 5% BSA for 1 h at room temperature, cells were incubated with anti-BrdU (Santa Cruz Biotechnology, Santa Cruz, CA, USA) and anti-Histone 3 (Proteintech, Wuhan, China) antibodies at 4°C overnight. Finally, the cell coverslips were incubated with proper secondary antibodies for 1 h at room temperature. The number of BrdU-positive cells was counted manually under a microscope in five random fields.[6]

Migration Assay

Migration assay was performed as previously described.[46] In brief, the migration test was performed in 24-mm Transwell with 8.0-μm pore polycarbonate membrane inserts (Corning, Corning, NY, USA). HUVECs transduced with lentiviral vectors were starved 12 h before migration assay. The Transwell chambers were coated with fibronectin (Sigma, Saint Louis, MO, USA) for at least 2 h. Extracellular matrix medium (ECM) (500 μL) was added to the lower compartment. HUVECs (2×10^4) suspended in serum-free and growth factors-free ECM were added to the upper chamber. After 24-h incubation, chambers were stained with crystal violet (Beyotime, Shanghai, China) for 10 min. The number of cells that migrated to the lower membrane surface was counted under a microscope (Leica Microsystems) in five random fields, and three wells were counted for each group.

Tube Formation Assay

Tube formation assay was performed as previously described.[47] In brief, Matrigel (50 μL; BD Biosciences, Franklin Lakes, NJ, USA) was added into 96-well plate and incubated at 37°C for 30 min. A total of 2×10^4 HUVECs transduced with LV-miRNA-126-3p, LV-miRNA-126-5p, LV-GPF, LV-miRNA-126-3p sponge, LV-miRNA-126-5p sponge, or LV-GFP sponge were suspended in 100 μL of ECM (Sciencell, San Diego, CA, USA) and seeded in the Matrigel-coated plate. After culturing for 3 h, the tube morphology was captured, five random fields per well, and three wells per group were counted. Tube length was measured and analyzed using ImageJ software.

Lentiviral Vector Brain Transduction

One week after pMCAO, mice were randomly divided into two groups and anesthetized with ketamine and xylazine and fixed on a stereotactic frame (RWD, Shenzhen, China). A total volume of 5 μL of LV-miRNA-126 (titer = 5.6×10^8/mL) or LV-GFP viral particles was injected stereotactically at a rate of 0.2 μL/min at 2 mm lateral to the bregma and 2.5 mm deep under the dura. The needle was maintained for 10 min before withdrawal. The bone hole was sealed with bone wax, and the wound was sutured. After awakening from anesthesia, the mice could return to their cages for long-term recovery.[48]

Brain Atrophy Volume Measurement

A series of 20-μm coronal sections was cut from the location that is anterior commissure to hippocampus. The distance between each section was 200 μm. The sections were stained using cresyl violet, and the atrophic area was calculated by subtracting the cresyl violet-stained area in the ipsilateral hemisphere from the whole area of the contralateral hemisphere using ImageJ software. The atrophy volume was calculated by the following formula: $= \sum_1^n [(S_n + \sqrt{S_n * S_{n+1}} + S_{n+1}) * h/3]$. Here S represents the atrophic area (mm^2) in each brain section, and h represents the adjacent brain slices height, here $h = 0.2$ mm.[12]

Neurobehavioral Tests

Two investigators who were blinded to the experimental groups performed neurobehavioral tests, including rotarod test and mNSSs. For rotarod test, mice were trained for 3 consecutive days prior to pMCAO surgery, and rotarod test was performed 1 day before pMCAO as baseline, and 1, 2, 3, and 4 weeks after pMCAO (0, 1, 2, and 3 weeks after virus injection). Mice were allowed 1-min adaption

Table 1. Real-Time PCR Primers

Gene	Forward Primer (5′–3′)	Reverse Primer (5′–3′)
DUSP10	CTCTGGTGTTGAAAGGTGGAC	TTGGAGCTGGAGGGAG TTGT
SPRED1	CTCAGGGACAAAATGGTGGTT	CCAGTGGTGAAATGTTG GAGT
PTPN9	ACAGTGACCAATCTAGGCGTG	TTTCTGCCGTTCCTCT GTGT
PTPN7	GGACATGAAAGAGTGCCCAGA	CCAGGCCGAAAAGAGG ATGT
PIK3R2	CACTCACCTTCTGCTCCGTT	TCTGGTCCTGCTGGTAT TTGG

period on the rod in rotarod test, after which the rod was accelerated to 40 revolutions per minute over 2 min; the time spent on the rod was recorded and analyzed.

mNSSs of the animals were graded on a scale of 0–14, which included motor, sensory, balance, and reflex tests (normal score, 0; maximal deficit score, 14).[49] mNSS test was performed at 1, 2, 3, and 4 weeks after pMCAO (0, 1, 2, and 3 weeks after viral vector injection).

Immunohistochemistry

Brains were post-fixed for 12 h with 4% paraformaldehyde, immersed in 30% sucrose until brains sunk to the bottom, then quickly frozen with isopentane. Brains were cut into 20-μm-thick coronal sections. Floating coronal sections were collected in antigen protective solution, which contained 20% glycol, 30% glycerol, and 50% PBS.

BrdU (50 mg/kg intraperitoneally doses given 8 h apart) was administered 1 week prior to mice sacrifice, and mice were sacrificed 2 and 3 weeks after stereotactic injection. For BrdU staining, sections were first fixed with 4% paraformaldehyde. The sections were treated with 0.3% Triton X-100 in PBS for 20 min and 1N HCl for 30 min at 37°C. The sections were then neutralized with sodium borate twice for 10 min in each. Sections were blocked by 5% BSA for 1 h at room temperature and incubated with anti-CD31 (R&D Systems), anti-DCX (Santa Cruz Biotechnology, Santa Cruz, CA, USA), and anti-BrdU antibodies at 4°C overnight. Finally, the sections were incubated with proper secondary antibodies for 1 h at room temperature.

To quantify the length and diameter of blood vessels, three fields were randomly selected from the perifocal region in each section, and five sections were calculated from each animal. Vessel length and diameter were measured by ImageJ software. Total vessel length per field, average vessel diameter, and the number of $CD31^+/BrdU^+$ cells in the perifocal region were compared to determine angiogenesis and vessel remodeling. The number of $DCX^+/BrdU^+$ cells in SVZ and perifocal region were quantified for neurogenesis.[19] To localize the PTPN9 expression, we double stained brain sections with PTPN9 (R&D Systems, Minneapolis, MN, USA) and NeuN (Millipore, Temecula, CA, USA), PTPN9, and CD31 (R&D Systems).

Real-Time PCR

Regional brain tissues from the ipsilateral hemisphere of ischemic mice (infarct hemisphere), including cortex and striatum, were isolated for real-time PCR to determine the mRNA levels of miRNA-126-3p and miRNA-126-5p target genes including *DUSP10*, *SPRED1*, *PTPN9*, *PTPN7*, and *PIK3R2*. RNA (300–500 ng) was used for the reverse transcription reaction with PrimeScript RT reagent kit according to the manufacturer's instruction (Takara, Dalian, China). The cDNA was quantified with StarScript II SYBR Two-Step qRT-PCR Synthesis Kit (Genstar, Beijing, China). The amplification parameters were under the following conditions: 95°C for 30 s followed by 40 cycles of 95°C for 5 s, and 60°C for 30 s. The primer sequences are listed in Table 1.

Western Blot Analysis

Brain tissues from the ipsilateral hemisphere of ischemic mice (infarct hemisphere), including cortex and striatum, were sonicated in homogenizing buffer, including radioimmunoprecipitation assay buffer (RIPA) lysis buffer (Millipore, Temecula, CA, USA), protease cocktail inhibitor (Thermo Fisher, Waltham, MA, USA), phosphatase inhibitor (Roche, Basel, Switzerland), and phenylmethanesulfonyl fluoride (Sigma, Saint Louis, MO, USA). Protein samples were loaded onto 10% resolving gel and incubated with primary antibodies including PTPN9 (1:1,000 dilution; Proteintech, Rosemont, IL, USA); p-AKT, AKT, p-ERK, ERK (1:1,000 dilution; Cell Signaling Technology, Danvers, MA, USA); and β-actin (1:1,000 dilution; Invitrogen, Carlsbad, CA, USA).

Dual-Luciferase Gene Reporter Assay

3′ UTR and mutant 3′ UTR of mouse PTPN9 were amplified and cloned into a pGL3 vector containing the firefly luciferase reporter gene (ObiO, Shanghai, China). For the dual-luciferase gene reporter assay, 293T cells were co-transfected with 0.1 μg of firefly luciferase constructs, 0.01 μg of pRL-TK renilla luciferase plasmid, and 100 nmol/L synthetic miRNA-126-3p, miRNA-126-5p mimic molecular, or mimic control molecular. Luciferase activity was measured using a dual-luciferase gene reporter assay (Promega, Madison, WI, USA) 48 h after transfection. The results were calculated as relative luciferase activity (firefly luciferase/renilla luciferase).

Statistical Analysis

Data from different groups were compared using one-way ANOVA followed by Tukey's post-tests or t test using SPSS 18.0 (SPSS, Armonk, NY, USA). All data were presented as mean ± SD or median with 95% confidence interval (CI). A p value <0.05 was considered statistically significant.

SUPPLEMENTAL INFORMATION

Supplemental Information includes six figures and can be found with this article online at https://doi.org/10.1016/j.omtn.2019.02.002.

AUTHOR CONTRIBUTIONS

M.Q. designed and performed the experiments, analyzed the data, and drafted the manuscript and figures. G.-Y.Y. and Y.T. conceived

the project, designed the experiments, and edited the paper finally. J.P. participated in the design of the study and contributed to virus brain injection and behavior tests. L.W. contributed to the animal model. P.Z. and Y.S. contributed to the western blot and mRNA analysis. S.W. contributed to the behavior test. L.J. contributed to data analysis. Z.Z. and Y.W. helped to design the experiment and interpret the data.

CONFLICTS OF INTEREST

The authors declare no competing interests.

ACKNOWLEDGMENTS

This study was supported by research grants from the National Natural Science Foundation of China (81771251 to G.-Y.Y., 81801170 to Y.T., 81771244 to Z.Z., and 81870921 to Y.W.), National Key Research and Development Program of China (2016YFC1300600), the K. C. Wong Education Foundation (to G.-Y.Y.), and the Science and Technology Commission of Shanghai Municipality (17ZR1413600 to Z.Z.).

REFERENCES

1. Cai, M., Zhang, W., Weng, Z., Stetler, R.A., Jiang, X., Shi, Y., Gao, Y., and Chen, J. (2017). Promoting neurovascular recovery in aged mice after ischemic stroke—prophylactic effect of omega-3 polyunsaturated fatty acids. Aging Dis. *8*, 531–545.
2. Prabhakaran, S., Ruff, I., and Bernstein, R.A. (2015). Acute stroke intervention: a systematic review. JAMA *313*, 1451–1462.
3. Ren, C., Wang, B., Li, N., Jin, K., and Ji, X. (2015). Herbal formula Danggui-Shaoyao-San promotes neurogenesis and angiogenesis in rat following middle cerebral artery occlusion. Aging Dis. *6*, 245–253.
4. Fan, Y., and Yang, G.Y. (2007). Therapeutic angiogenesis for brain ischemia: a brief review. J. Neuroimmune Pharmacol. *2*, 284–289.
5. Tang, Y., Wang, L., Wang, J., Lin, X., Wang, Y., Jin, K., and Yang, G.Y. (2015). Ischemia-induced angiogenesis is attenuated in aged rats. Aging Dis. *7*, 326–335.
6. Tang, Y., Wang, J., Lin, X., Wang, L., Shao, B., Jin, K., Wang, Y., and Yang, G.Y. (2014). Neural stem cell protects aged rat brain from ischemia-reperfusion injury through neurogenesis and angiogenesis. J. Cereb. Blood Flow Metab. *34*, 1138–1147.
7. Shen, F., Su, H., Fan, Y., Chen, Y., Zhu, Y., Liu, W., Young, W.L., and Yang, G.Y. (2006). Adeno-associated viral-vector-mediated hypoxia-inducible vascular endothelial growth factor gene expression attenuates ischemic brain injury after focal cerebral ischemia in mice. Stroke *37*, 2601–2606.
8. Sbarbati, A., Pietra, C., Baldassarri, A.M., Guerrini, U., Ziviani, L., Reggiani, A., Boicelli, A., and Osculati, F. (1996). The microvascular system in ischemic cortical lesions. Acta Neuropathol. *92*, 56–63.
9. Gunsilius, E., Petzer, A.L., Stockhammer, G., Kähler, C.M., and Gastl, G. (2001). Serial measurement of vascular endothelial growth factor and transforming growth factor-beta1 in serum of patients with acute ischemic stroke. Stroke *32*, 275–278.
10. Li, J., Tang, Y., Wang, Y., Tang, R., Jiang, W., Yang, G.Y., and Gao, W.Q. (2014). Neurovascular recovery via co-transplanted neural and vascular progenitors leads to improved functional restoration after ischemic stroke in rats. Stem Cell Reports *3*, 101–114.
11. Lu, H., Wang, Y., He, X., Yuan, F., Lin, X., Xie, B., Tang, G., Huang, J., Tang, Y., Jin, K., et al. (2012). Netrin-1 hyperexpression in mouse brain promotes angiogenesis and long-term neurological recovery after transient focal ischemia. Stroke *43*, 838–843.
12. Li, Y., Huang, J., He, X., Tang, G., Tang, Y.H., Liu, Y., Lin, X., Lu, Y., Yang, G.Y., and Wang, Y. (2014). Postacute stromal cell-derived factor-1α expression promotes neurovascular recovery in ischemic mice. Stroke *45*, 1822–1829.
13. Sun, H., Le, T., Chang, T.T., Habib, A., Wu, S., Shen, F., Young, W.L., Su, H., and Liu, J. (2011). AAV-mediated netrin-1 overexpression increases peri-infarct blood vessel density and improves motor function recovery after experimental stroke. Neurobiol. Dis. *44*, 73–83.
14. Fan, Y., Shen, F., Chen, Y., Hao, Q., Liu, W., Su, H., Young, W.L., and Yang, G.Y. (2008). Overexpression of netrin-1 induces neovascularization in the adult mouse brain. J. Cereb. Blood Flow Metab. *28*, 1543–1551.
15. Zhu, W., Fan, Y., Frenzel, T., Gasmi, M., Bartus, R.T., Young, W.L., Yang, G.Y., and Chen, Y. (2008). Insulin growth factor-1 gene transfer enhances neurovascular remodeling and improves long-term stroke outcome in mice. Stroke *39*, 1254–1261.
16. Zeng, L., He, X., Wang, Y., Tang, Y., Zheng, C., Cai, H., Liu, J., Wang, Y., Fu, Y., and Yang, G.Y. (2014). MicroRNA-210 overexpression induces angiogenesis and neurogenesis in the normal adult mouse brain. Gene Ther. *21*, 37–43.
17. Chen, J., Zhang, Z.G., Li, Y., Wang, L., Xu, Y.X., Gautam, S.C., Lu, M., Zhu, Z., and Chopp, M. (2003). Intravenous administration of human bone marrow stromal cells induces angiogenesis in the ischemic boundary zone after stroke in rats. Circ. Res. *92*, 692–699.
18. Fan, Y., Shen, F., Frenzel, T., Zhu, W., Ye, J., Liu, J., Chen, Y., Su, H., Young, W.L., and Yang, G.Y. (2010). Endothelial progenitor cell transplantation improves long-term stroke outcome in mice. Ann. Neurol. *67*, 488–497.
19. Tang, Y., Cai, B., Yuan, F., He, X., Lin, X., Wang, J., Wang, Y., and Yang, G.Y. (2014). Melatonin pretreatment improves the survival and function of transplanted mesenchymal stem cells after focal cerebral ischemia. Cell Transplant. *23*, 1279–1291.
20. Zeng, L.L., He, X.S., Liu, J.R., Zheng, C.B., Wang, Y.T., and Yang, G.Y. (2016). Lentivirus-mediated overexpression of microRNA-210 improves long-term outcomes after focal cerebral ischemia in mice. CNS Neurosci. Ther. *22*, 961–969.
21. Schober, A., Nazari-Jahantigh, M., Wei, Y., Bidzhekov, K., Gremse, F., Grommes, J., Megens, R.T., Heyll, K., Noels, H., Hristov, M., et al. (2014). MicroRNA-126-5p promotes endothelial proliferation and limits atherosclerosis by suppressing Dlk1. Nat. Med. *20*, 368–376.
22. DA Silva, N.D., Jr., Fernandes, T., Soci, U.P., Monteiro, A.W., Phillips, M.I., and DE Oliveira, E.M. (2012). Swimming training in rats increases cardiac MicroRNA-126 expression and angiogenesis. Med. Sci. Sports Exerc. *44*, 1453–1462.
23. Luo, Q., Guo, D., Liu, G., Chen, G., Hang, M., and Jin, M. (2017). Exosomes from miR-126-overexpressing ADSCs are therapeutic in relieving acute myocardial ischaemic injury. Cell. Physiol. Biochem. *44*, 2105–2116.
24. Liu, J., Wang, Y., Akamatsu, Y., Lee, C.C., Stetler, R.A., Lawton, M.T., and Yang, G.Y. (2014). Vascular remodeling after ischemic stroke: mechanisms and therapeutic potentials. Prog. Neurobiol. *115*, 138–156.
25. Zhou, Q., Anderson, C., Hanus, J., Zhao, F., Ma, J., Yoshimura, A., and Wang, S. (2016). Strand and cell type-specific function of microRNA-126 in angiogenesis. Mol. Ther. *24*, 1823–1835.
26. Cao, W.J., Rosenblat, J.D., Roth, N.C., Kuliszewski, M.A., Matkar, P.N., Rudenko, D., Liao, C., Lee, P.J., and Leong-Poi, H. (2015). Therapeutic angiogenesis by ultrasound-mediated microRNA-126-3p delivery. Arterioscler. Thromb. Vasc. Biol. *35*, 2401–2411.
27. Nichols-Larsen, D.S., Clark, P.C., Zeringue, A., Greenspan, A., and Blanton, S. (2005). Factors influencing stroke survivors' quality of life during subacute recovery. Stroke *36*, 1480–1484.
28. Mathiyalagan, P., Liang, Y., Kim, D., Misener, S., Thorne, T., Kamide, C.E., Klyachko, E., Losordo, D.W., Hajjar, R.J., and Sahoo, S. (2017). Angiogenic mechanisms of human $CD34^{+}$ stem cell exosomes in the repair of ischemic hindlimb. Circ. Res. *120*, 1466–1476.
29. Huang, F., Zhu, X., Hu, X.Q., Fang, Z.F., Tang, L., Lu, X.L., and Zhou, S.H. (2013). Mesenchymal stem cells modified with miR-126 release angiogenic factors and activate Notch ligand Delta-like-4, enhancing ischemic angiogenesis and cell survival. Int. J. Mol. Med. *31*, 484–492.
30. Xiong, Y., Mahmood, A., and Chopp, M. (2010). Angiogenesis, neurogenesis and brain recovery of function following injury. Curr. Opin. Investig. Drugs *11*, 298–308.
31. Font, M.A., Arboix, A., and Krupinski, J. (2010). Angiogenesis, neurogenesis and neuroplasticity in ischemic stroke. Curr. Cardiol. Rev. *6*, 238–244.
32. Zhang, R., Zhang, Z., Wang, L., Wang, Y., Gousev, A., Zhang, L., Ho, K.L., Morshead, C., and Chopp, M. (2004). Activated neural stem cells contribute to stroke-induced neurogenesis and neuroblast migration toward the infarct boundary in adult rats. J. Cereb. Blood Flow Metab. *24*, 441–448.

33. Lu, J., Manaenko, A., and Hu, Q. (2017). Targeting adult neurogenesis for poststroke therapy. Stem Cells Int. *2017*, 5868632.

34. Chopp, M., Zhang, Z.G., and Jiang, Q. (2007). Neurogenesis, angiogenesis, and MRI indices of functional recovery from stroke. Stroke *38* (*Suppl 2*), 827–831.

35. Fish, J.E., Santoro, M.M., Morton, S.U., Yu, S., Yeh, R.F., Wythe, J.D., Ivey, K.N., Bruneau, B.G., Stainier, D.Y., and Srivastava, D. (2008). miR-126 regulates angiogenic signaling and vascular integrity. Dev. Cell *15*, 272–284.

36. Song, Z.Y., Wang, F., Cui, S.X., and Qu, X.J. (2018). Knockdown of CXCR4 inhibits CXCL12-induced angiogenesis in HUVECs through downregulation of the MAPK/ERK and PI3K/AKT and the Wnt/β-catenin pathways. Cancer Invest. *36*, 10–18.

37. Le Belle, J.E., Orozco, N.M., Paucar, A.A., Saxe, J.P., Mottahedeh, J., Pyle, A.D., Wu, H., and Kornblum, H.I. (2011). Proliferative neural stem cells have high endogenous ROS levels that regulate self-renewal and neurogenesis in a PI3K/Akt-dependant manner. Cell Stem Cell *8*, 59–71.

38. Xiao, Z., Kong, Y., Yang, S., Li, M., Wen, J., and Li, L. (2007). Upregulation of Flk-1 by bFGF via the ERK pathway is essential for VEGF-mediated promotion of neural stem cell proliferation. Cell Res. *17*, 73–79.

39. van Solingen, C., de Boer, H.C., Bijkerk, R., Monge, M., van Oeveren-Rietdijk, A.M., Seghers, L., de Vries, M.R., van der Veer, E.P., Quax, P.H., Rabelink, T.J., and van Zonneveld, A.J. (2011). MicroRNA-126 modulates endothelial SDF-1 expression and mobilization of Sca-1(+)/Lin(-) progenitor cells in ischaemia. Cardiovasc. Res. *92*, 449–455.

40. Neel, B.G., and Tonks, N.K. (2016). Protein Tyrosine Phosphatases in Cancer (Springer New York).

41. Alonso, A., Sasin, J., Bottini, N., Friedberg, I., Friedberg, I., Osterman, A., Godzik, A., Hunter, T., Dixon, J., and Mustelin, T. (2004). Protein tyrosine phosphatases in the human genome. Cell *117*, 699–711.

42. Yao, T.W., Zhang, J., Prados, M., Weiss, W.A., James, C.D., and Nicolaides, T. (2015). EGFR blockade prevents glioma escape from BRAFV600E targeted therapy. Oncotarget *6*, 21993–22005.

43. Kappert, K., Peters, K.G., Böhmer, F.D., and Ostman, A. (2005). Tyrosine phosphatases in vessel wall signaling. Cardiovasc. Res. *65*, 587–598.

44. Huang, J., Li, Y., Tang, Y., Tang, G., Yang, G.Y., and Wang, Y. (2013). CXCR4 antagonist AMD3100 protects blood-brain barrier integrity and reduces inflammatory response after focal ischemia in mice. Stroke *44*, 190–197.

45. Chang, S., Li, Y., Yuan, F., Qu, M., Song, Y., Zhang, Z., Yang, G.Y., and Wang, Y. (2017). Monomeric CXCL12 outperforms its dimeric and wild type variants in the promotion of human endothelial progenitor cells' function. Biochem. Biophys. Res. Commun. *488*, 303–310.

46. Fan, Y., Ye, J., Shen, F., Zhu, Y., Yeghiazarians, Y., Zhu, W., Chen, Y., Lawton, M.T., Young, W.L., and Yang, G.Y. (2008). Interleukin-6 stimulates circulating blood-derived endothelial progenitor cell angiogenesis in vitro. J. Cereb. Blood Flow Metab. *28*, 90–98.

47. Huang, J., Song, J., Qu, M., Wang, Y., An, Q., Song, Y., Yan, W., Wang, B., Wang, X., Zhang, S., et al. (2017). MicroRNA-137 and microRNA-195* inhibit vasculogenesis in brain arteriovenous malformations. Ann. Neurol. *82*, 371–384.

48. Wang, Y., Huang, J., Ma, Y., Tang, G., Liu, Y., Chen, X., Zhang, Z., Zeng, L., Wang, Y., Ouyang, Y.B., and Yang, G.Y. (2015). MicroRNA-29b is a therapeutic target in cerebral ischemia associated with aquaporin 4. J. Cereb. Blood Flow Metab. *35*, 1977–1984.

49. Li, Y., Chopp, M., Chen, J., Wang, L., Gautam, S.C., Xu, Y.X., and Zhang, Z. (2000). Intrastriatal transplantation of bone marrow nonhematopoietic cells improves functional recovery after stroke in adult mice. J. Cereb. Blood Flow Metab. *20*, 1311–1319.